



Investigation into the effectiveness of ultrasound SHI imaging according to static and dynamic parameters of contrast agents

F. Lin, F. Varray, C. Cachard and O. Basset

Centre de recherche en applications et traitement de l'image pour la santé, 7 avenue Jean
Capelle, Bat Blaise Pascal, 69621 Villeurbanne Cedex
fanglue.lin@creatis.insa-lyon.fr

Second harmonic inversion (SHI) is a new method to improve contrast to tissue ratio (CTR) of ultrasound contrast images through reducing tissue-generated 2nd harmonics during wave propagation. Two 90° phase-shifted pulses with the same frequencies and amplitudes are transmitted. The two received RF data are summed and filtered around 2nd harmonic frequency to create SHI image. However, after experimental evaluation on SHI's effectiveness, we found that movements and destruction of contrast agent bubbles strongly affect the results of SHI. Using CREANUIS software, SHI is simulated with various bubble movements (Δd), reflective amplitude (Amp) and medium's nonlinear parameter (β) changes. Amp and β decreasing are two different ways to describe the bubble cloud evolution. The influences are quantified by CTR of SHI images. Simulation results show that CTR improves by 11dB for 100% β destruction and 13dB for 100% Amp destruction. In lateral direction, CTR rises until reaching a stable value when bubble movement increases between the two pulses. In axial direction, CTR exhibits oscillations with increasing movements with respect to transmitted pulse wavelength. The maximum increases are both 16dB. So SHI is expected to be optimized by increasing the power and adjusting pulse repetition frequency (PRF) of transmitted pulses.

1 Introduction

Ultrasound contrast agents (UCAs) are micro-bubbles with diameters of a few micrometers. They are used to improve the detection of blood flow and perfused tissue due to the enhanced back-scattered echoes from micro-bubbles which are injected into the blood vessel [1]. In fact, the backscattered echoes also have harmonics because of the asymmetric vibration of these micro-bubbles when exposed to the ultrasound pressures [2][3]. Therefore, these harmonics can be extracted to form ultrasound harmonic images, which aim to distinguish blood pool and tissue. Second harmonic imaging is the most common adopted because of the limited bandwidth of the traditional transducer.

However, if a one-cycle pulse, that is a broad-band pulse, is transmitted, there is inevitable spectral overlap between the fundamental and harmonic frequencies. To increase the sensitivity of the system in detecting agents, a multiple-cycle pulse, that is a narrow-band pulse, have to be transmitted, which nevertheless deteriorate the imaging resolution. Therefore, there exists the contrast detectability and imaging resolution trade-off in classic harmonic imaging [4].

In order to overcome this trade-off, a technique called pulse inversion (PI) has been proposed [5]. A sequence of inverted two pulses is transmitted. For a linear system, the response of the second pulse is an inverted copy of the response from the first pulse and the sum of the two pulses is zero. For a nonlinear system, the sum is not zero. Pulse inversion works over the entire bandwidth of the received echo signal and achieves better image resolution. However, it was finally found that tissue can also generate harmonics because the transmitted wave is deformed gradually during the propagation in tissue [6]. Therefore, the contrast-to-tissue ratio (CTR) is limited because of tissue-generated harmonics. CTR is used to quantify the extent of discrimination between UCA and tissue, which is defined for each harmonic as:

$$CTR_n = 20 \log \frac{P_n^{UCA}}{P_n^{tissue}} \quad (1)$$

where P_n^{UCA} and P_n^{tissue} are backscattered pressures of n^{th} harmonic from UCA and tissue, respectively.

Eq. (1) claims that to increase CTR_2 in contrast harmonic imaging, the 2nd harmonic generated by tissue should be reduced and the 2nd harmonic produced by UCA should be enhanced. Several techniques have been proposed to suppress the 2nd harmonic generated by tissue.

Most of them used one source pre-biasing signal in transmission. The differences between these techniques stay in how this source pre-biasing signal is designed [7][8][9][10].

Pasovic *et al* proposed a method called second harmonic inversion (SHI) [11]. Like in PI, a sequence of two pulses is transmitted and the two responses are summed, but the phase shift between the two transmitted pulses is 90°. Because the second harmonic component has a quadratic relationship to the fundamental one, the phase shift between the two second harmonic components is 180°, so the second harmonic is well cancelled in tissue. In the contrast agent region, a good preservation of second harmonic was observed (maximum reduction was only 0.3 dB), therefore, the CTR is effectively increased. The preservation of second harmonic was explained as Morgan [12] observed that the reflected signals by a single bubble excited by a couple of inverted one-cycle pulses had frequency shift and the polarities of the two received echo were not significantly changed. However, it could be also because of the movement of the bubbles considering that the UCA were always stirred during the acquisitions and the destruction of UCA because the transmitted energy was relatively high.

Considering the effects like resonance, cavitation and so on, the reflection of a single bubble to US wave is complex, needless to say a cloud of bubbles. Therefore, the quantification of influence of UCA movement and destruction is interesting and useful for the optimization of SHI.

This paper is a preliminary study of the influence of UCA movement and destruction when tissue and UCA are impacted by two ultrasonic waves with 90° phase shift. In this paper, bubble cloud is regarded as a group of stronger reflectors with higher nonlinear parameter. SHI is simulated with various bubble movements (Δd), reflective amplitude (Amp) and medium's nonlinear parameter (β) changes. Amp and β decreasing are two different ways to describe the bubble cloud evolution. The influences are quantified by CTR of SHI images.

The paper is organized as follows: Part 2 introduces the theoretical background. Part 3 presents the simulation results of SHI on static bubbles, moving bubbles and destructed bubbles respectively. Part 4 discusses and concludes this paper.

2 Theory

The complete model of nonlinear wave propagation in tissue can be described by the Khokhlov Zabolotskaya Kuznetsov (KZK) equation [13]:

$$\frac{\partial^2 p}{\partial z \partial t} = \frac{c_0}{2} \Delta^2 p + \frac{\delta}{2c_0^3} \frac{\partial^3 p}{\partial t^3} + \frac{\beta}{2\rho_0 c_0^3} \frac{\partial^2 p^2}{\partial t^2} \quad (2)$$

where p is the transmitted pressure, z is the propagating distance, t is the propagating time, c_0 is the speed of sound, δ is the attenuation of the medium, ρ_0 is the density of the medium and β is the nonlinearity coefficient of the medium. The first term of the right side of Eq. (2) means diffraction effect of the probe, the second terms stands for the absorption of the medium and the last term represents the nonlinear distortion of the medium. If the diffraction effect is ignored, the KZK equation becomes the Burger equation, which describes the plane wave propagation. Furthermore, for a non-viscous homogeneous medium, a lossless Burger equation can be written as [14]:

$$\frac{\partial p}{\partial z} = \frac{\beta}{2\rho_0 c_0^3} \frac{\partial^2 p^2}{\partial t^2} \quad (3)$$

Assuming the two successively transmitted pulses are:

$$p_1(z=0, t) = P \cos(\omega t + \varphi_1) \quad (4)$$

$$p_2(z=0, t) = P \cos(\omega t + \varphi_2) \quad (5)$$

where P is the amplitude of the pulse, ω is the angular frequency, φ_1 and φ_2 are the phases.

After propagating some distance z in the medium, harmonics appear as described by Eq. (2) and the pressure is:

$$p_1(z, t) = P \sum_{n=1}^{\infty} \frac{2J_n(n\ell_D)}{n\ell_D} \cos(n(\omega t + \varphi_1)) \quad (6)$$

$$p_2(z, t) = P \sum_{n=1}^{\infty} \frac{2J_n(n\ell_D)}{n\ell_D} \cos(n(\omega t + \varphi_2)) \quad (7)$$

Where

$$\ell_D = \frac{\omega P}{\rho_0 c_0^3} z \quad (8)$$

J_n is the n^{th} order Bessel function of the first kind, ℓ_D is the normalized dimensionless propagation distance. Note that ℓ_D depends on the amplitude and frequency of the transmitted wave, the properties of the medium and the propagating distance.

Let:

$$\Delta\varphi = \varphi_2 - \varphi_1 \quad (9)$$

Using trigonometric properties, the summation of the two waves can be expressed as:

$$p_{\text{sum}}(z, t) = 4P \sum_{n=1}^{\infty} \frac{J_n(n\ell_D)}{n\ell_D} \cos(n(\omega t + \varphi_1 + \frac{\Delta\varphi}{2})) \cdot \cos(\frac{n\Delta\varphi}{2}) \quad (10)$$

Therefore, when

$$n = \frac{k\pi}{\Delta\varphi}, \text{ where } k = 1, 3, 5... \quad (11)$$

n^{th} harmonic is zero.

When

$$n = \frac{2k\pi}{\Delta\varphi}, \text{ where } k = 1, 2, 3... \quad (12)$$

n^{th} harmonic doubles.

Therefore, for PI ($\Delta\varphi = \pi$), every odd harmonic is zero

and every even harmonic doubles. For SHI ($\Delta\varphi = \frac{\pi}{2}$), every $4j+2$ harmonic is zero, where $j = 0, 1, 2...$

3 Simulations

To simulate the response of a static cloud of bubbles excited by transmitted pulses with 90° phase shift and the influence of bubble movements and bubble destruction, a new nonlinear simulator CREANUIS is used [15]. It is a tool that simulates nonlinear radio frequency (RF) ultrasound images. It is the combination of two specific tools. The former is a nonlinear ultrasound propagation simulator, that allows compute the evolution of the fundamental and second harmonic wave. Then, using this field information, a reconstruction algorithm is used to create the corresponding nonlinear radio frequency (RF) image. The resulting RF image contains not only the fundamental evolution, but also the second harmonic one. With the design of nonlinear propagation simulator, which is a generalization of angular spectrum method (GASM), media with an inhomogeneous nonlinear coefficient can be quickly simulated.

3.1 Static medium

Two pulses with 90° phase shifts are transmitted. The two pulses have a central frequency of 3 MHz, an initial pressure of 100 kPa and cycle of 3. The image depth is 50 mm. The focal depth is 40 mm.

Two parameters (Amp and β) are used to describe the medium. The parameters of the tissue are set to be totally the same through all the simulations in order to simulate a static tissue. β of tissue is set to be 5, which is a typical value for homogeneous tissue medium. β of bubble cloud is set to be 51. The amplitude of each reflector in bubble region is set to be 30 times larger than that in tissue region. The bubble region is a cubical shape whose long axis is parallel or perpendicular to the wave propagation direction.

For each transmitted wave, one RF image is created. The two RF images corresponding to two transmitted waves are summed. The 2nd harmonic signals from the summed signals are filtered to form images, which are referred as SHI images. Figure 1 compares the classic harmonic image and SHI image. Figure 2 shows the frequency spectrum of the RF signal from one excitation pulse and that of summed signal from two excitation pulses with 90° phase shift in tissue region and contrast agents region respectively.

Figure 1 indicates that on static bubble cloud, the effect of SHI is not evident. That is, the discrimination between contrast agents and tissue is not obvious. That can be explained in Figure 2, the 2nd harmonic in contrast agents region is also reduced unexpectedly although the 2nd harmonic in tissue region is effectively suppressed.

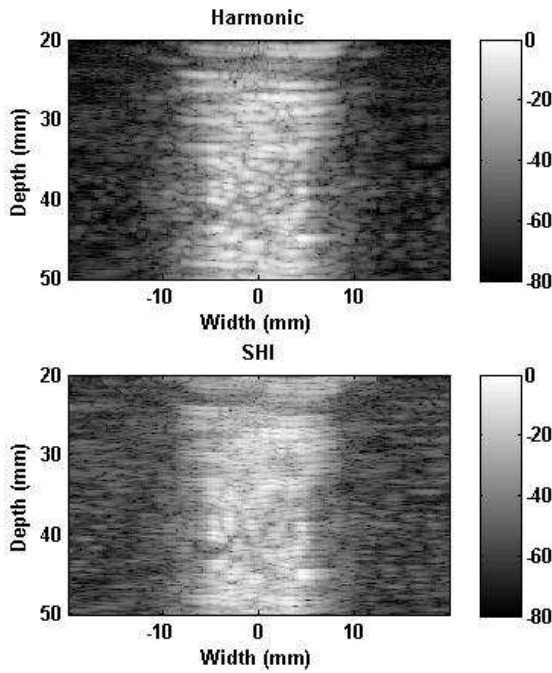


Figure 1: Comparison of the classic harmonic image (upper) and SHI image (lower).

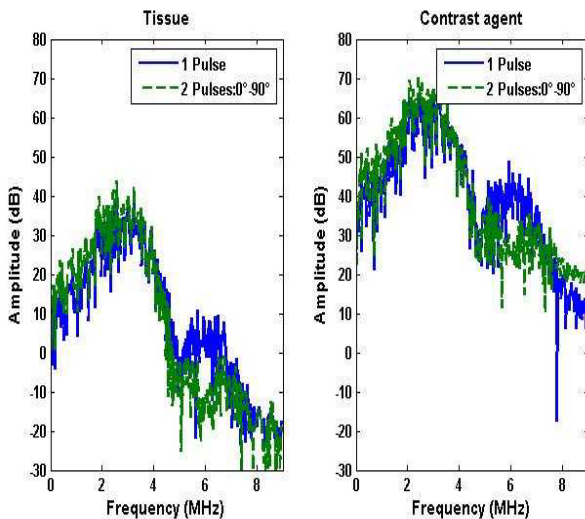


Figure 2: Frequency spectrum of the RF signal from one excitation pulse (solid line) and that of summed signal from two excitation pulses with 90° phase shift (dashed line). The transmitted frequency is 3 MHz.

3.2 Bubble movement

The influence of bubble movement to the effectiveness of SHI method is then studied, considering that bubbles always move with blood in real life.

The simulations of bubble movements are conducted with two cases: one, both the long axis and the movement direction of the bubble cloud are parallel with the wave propagation direction (referred as axial direction); the other, both the two are perpendicular with the propagation direction (referred as lateral direction).

Before the 2nd pulse is transmitted, the reflectors within the contrast agent region are relocated with the displacement in axial direction or lateral direction from the initial positions ranging from 0 to 0.5 mm (the wavelength λ of the transmitted pulse). For each displacement, SHI

images are formed and CTR are calculated. Figure 3 presents the tendency of CTR with increasing bubble displacements in axial and lateral directions, respectively.

Figure 3 shows that in axial direction, CTR exhibits oscillations. The movements produce an additional phase shift on the reflected signals. With the movement of $\lambda/8$, CTR reaches the maximum. That is because $\lambda/8$ leads to an addition 90° phase shift on the received signals. The total 180° phase shift makes the 2nd harmonic of summation doubles compared to the 2nd harmonic obtained with one pulse. In lateral direction, CTR also rises. The maximum increases for the two directions are about 16 dB. Figure 4 compares the SHI image without movement and that with movement of $\lambda/8$. The latter has a much larger discrimination between contrast agents and tissue than the former.

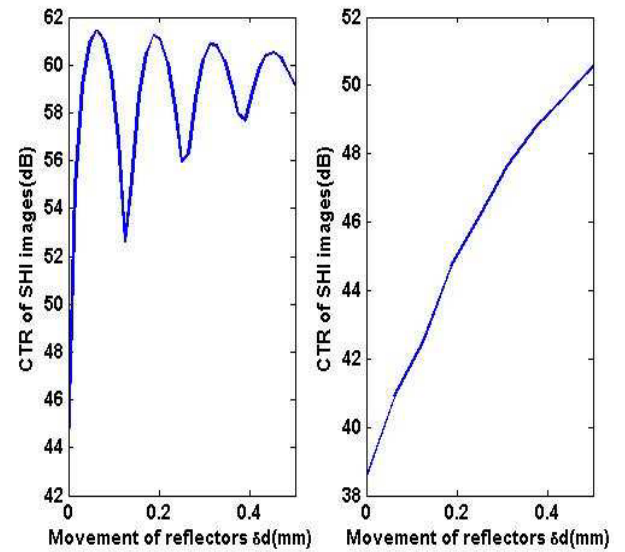


Figure 3: The tendency of CTR of SHI images with increasing bubble displacements between two transmitted pulses in axial (left) and lateral (right) direction.

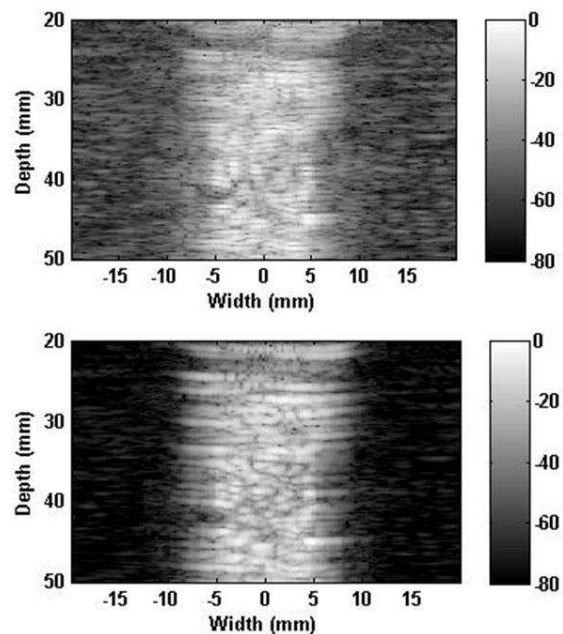


Figure 4: Comparison of the SHI image without movement (upper) and that with movement of $\lambda/8$ (lower).

3.3 Bubble destruction

As mentioned above, two parameters, β and Amp, are used to describe the properties of the medium. Bubble reflectors have larger values for the two parameters. Before the 2nd pulse is transmitted, in order to simulate the disappearance of the bubbles, one of the parameters (β and Amp) of certain percentage of the bubble reflectors are given smaller values. Then SHI image is formed and CTR is calculated. Figure 5 is the CTR variation with the increasing “ β decrease” percentage and “Amp decrease” percentage of bubble cloud. The CTR variations in axial direction and lateral direction are presented. Figure 6 compares the SHI image without any destruction and that with the total (100%) Amp destruction.

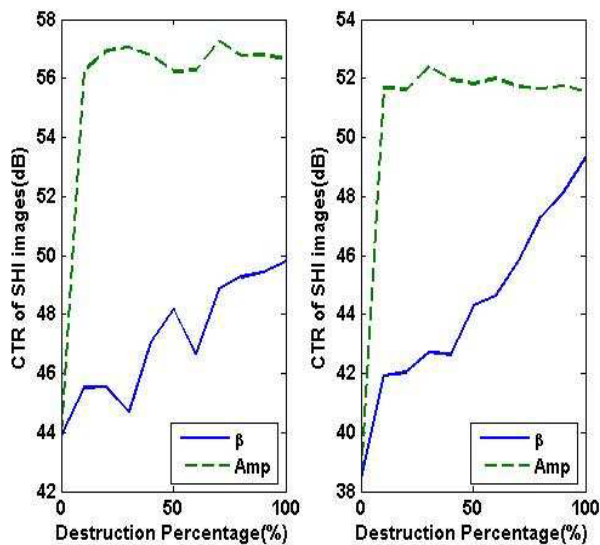


Figure 5: CTR variation with the increasing β decrease percentage (solid line) and Amp decrease (dotted line) percentage of bubble cloud. The CTR variations in axial direction (left) and lateral direction (right) are presented.

Figure 5 and Figure 6 demonstrate that with increasing bubble destruction, the effectiveness of SHI method should be better. In axial direction, CTR is improved by 6 dB for 100% β destruction and 12 dB for 100% Amp destruction. In lateral direction, CTR is increased by 11 dB for 100% β destruction and 13 dB for 100% Amp destruction. In real life, the decrease of β and Amp of bubbles occurs at the same time, which should lead to more rapid destruction, so larger CTR increase as well.

4 Conclusion and discussion

On static bubble cloud, the effectiveness of SHI is degraded because of the reduction of 2nd harmonic in contrast agents region. With bubble movement and bubble destruction, the effectiveness of SHI can be guaranteed even improved. Therefore SHI is expected to be optimized by increasing the transmitted power and adjusting pulse repetition frequency (PRF) of transmitted pulses.

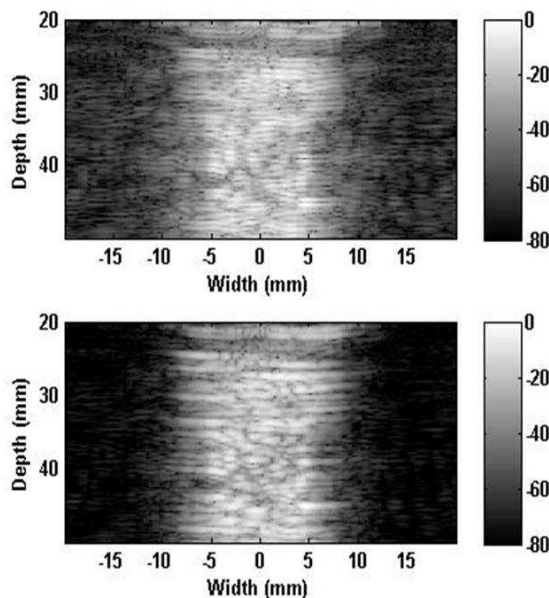


Figure 6: Comparison of the SHI image without any destruction (upper) and that with the total (100%) Amp destruction (lower).

Acknowledgments

This work has been partially supported by Centre Lyonnais d'Acoustique (CeLyA), ANR grant n°2011-LABX-014

References

- [1] R. Gramiak and P. M. Shah, “Echocardiography of the aortic root,” *Investigative Radiology*, vol. 3, no. 5, pp. 356-366, 1968.
- [2] N. De Jong, R. Cornet, C. Lancee, and S. Diego, “Higher harmonics of vibrating gas-filled microspheres. Part one: simulations,” *Ultrasonics*, vol. 32, no. 6, pp. 447-453, 1994.
- [3] S. Diego, “Higher harmonics of vibrating gas-filled microspheres. Part two: measurements,” *Ultrasonics*, vol. 32, no. 6, pp. 455-459, 1994.
- [4] P. J. . Frinking, A. Bouakaz, J. Kirkhorn, F. J. Ten Cate, and N. de Jong, “Ultrasound contrast imaging: current and new potential methods,” *Ultrasound in Medicine & Biology*, vol. 26, no. 6, pp. 965-975, Jul. 2000.
- [5] D. H. Simpson, C. T. Chin, and P. N. Burns, “Pulse inversion Doppler: a new method for detecting nonlinear echoes from microbubble contrast agents,” *IEEE transactions on ultrasonics, ferroelectrics, and frequency control*, vol. 46, no. 2, pp. 372-82, Jan. 1999.
- [6] S. I. Aanonsen, T. Barkve, J. N. Tjøtta, and S. Tjøtta, “Distortion and harmonic generation in the nearfield of a finite amplitude sound beam,” *The Journal of the Acoustical Society of America*, vol. 75, no. 1984, p. 749, 1984.

- [7] S. Krishnan, J. D. Hamilton, and M. O'Donnell, "Suppression of propagating second harmonic in ultrasound contrast imaging," *Ultrasonics, Ferroelectrics and Frequency Control, IEEE Transactions on*, vol. 45, no. 3, pp. 704–711, 1998.
- [8] C. C. Shen, Y. C. Wang, and Y. C. Hsieh, "Third harmonic transmit phasing for tissue harmonic generation," *Ultrasonics, Ferroelectrics and Frequency Control, IEEE Transactions on*, vol. 54, no. 7, pp. 1370–1381, 2007.
- [9] C.-C. Shen and Y.-C. Hsieh, "Optimal transmit phasing on tissue background suppression in contrast harmonic imaging," *Ultrasound in medicine & biology*, vol. 34, no. 11, pp. 1820-31, Nov. 2008.
- [10] M. Pasovic et al., "Broadband reduction of the second harmonic distortion during nonlinear ultrasound wave propagation," *Ultrasound in medicine biology*, vol. 36, no. 10, pp. 1568-1580, 2010.
- [11] M. Pasovic et al., "Second harmonic inversion for ultrasound contrast harmonic imaging," *Physics in Medicine and Biology*, vol. 56, no. 11, p. 3163, Jun. 2011.
- [12] K. E. Morgan, M. Averkiou, and K. Ferrara, "The effect of the phase of transmission on contrast agent echoes," *IEEE transactions on ultrasonics, ferroelectrics, and frequency control*, vol. 45, no. 4, pp. 872-5, Jan. 1998.
- [13] E. A. Zabolotskaya and R. V. Khokhlov, "Quasi-plane waves in the nonlinear acoustics of confined beams," *Soviet Physics Acoustics*, vol. 15, pp. 35–40, 1969.
- [14] J. M. Burgers, "A mathematical model illustrating the theory of turbulence," *Advances In Applied Mechanics*, vol. 1, pp. 171-199, 1948.
- [15] F. Varray, A. Ramalli, C. Cachard, P. Tortoli, and O. Basset, "Fundamental and second-harmonic ultrasound field computation of inhomogeneous nonlinear medium with a generalized angular spectrum method," *IEEE Transactions on Ultrasonics, Ferroelectrics and Frequency Control*, vol. 58, no. 7, pp. 1366-1376, 2011.